



# Template-directed supramolecular assembly of a new type of nanoporous peptide-based material<sup>‡</sup>

CARL HENRIK GÖRBITZ\* and FRODE RISE

Department of Chemistry, University of Oslo, Blindern, N-0315 OSLO, Norway

Received 1 July 2007; Revised 17 October 2007; Accepted 22 October 2007

**Abstract:** Dipeptides with two hydrophobic residues are known to often form crystals with hydrophobic or hydrophilic channels. One of the exceptions is Leu-Ile, which has been previously shown to crystallize as a nonporous 0.75 hydrate in the hexagonal space group  $P6_1$  with  $Z' = 4$ . We have now found that in the presence of D-Leu, a second pseudopolymorph of the dipeptide is formed. The crystal structure has hydrophilic, water-filled channels with an irregular cross section of approximately  $5.5 \times 3.5 \text{ \AA}$  and constitutes the first example of a crystal packing arrangement where the direction of the channels is perpendicular to the direction of hydrophobic stacking of side chains rather than parallel as in all other porous peptide-based materials. Copyright © 2008 European Peptide Society and John Wiley & Sons, Ltd.

Supplementary electronic material for this paper is available in Wiley InterScience at <http://www.interscience.wiley.com/jpages/1075-2617/suppmat/>

**Keywords:** dipeptides; nanotube; template; self-assembly; supramolecular structure

## INTRODUCTION

Out of the 25 dipeptides that can be constructed from the five hydrophobic residues Ala, Val, Ile, Leu and Phe 12 have so far been shown to form nanoporous organic materials [1]. The crystal structures of these hydrophobic dipeptides may be divided into two different classes:

- The Val-Ala class with 3-D hydrogen bonding and hydrophobic pores. Hexagonal space group, usually  $P6_1$ . Promoted by Ala, Val, and Ile residues [2–4].
- The Phe-Phe class with 1-D hydrogen bonding and hydrophilic pores. Space group may be monoclinic, orthorhombic, tetragonal, or hexagonal. Promoted by Leu and Phe residues [5–8].

The two types of crystal packing arrangements are illustrated schematically in Figure 1.

One of the first hydrophobic dipeptides investigated was Leu-Val, which easily forms crystals of the 0.75 hydrate in the hexagonal space group  $P6_5$  with  $Z' = 4$  [9]. Crystallization of Leu-Ile, Scheme 1, is more challenging, but crystals were eventually formed by fast evaporation of an aqueous solution at elevated temperature, and proved to be isostructural to Leu-Val [10]. Figure 2 illustrates how the hydrophobic side

chains aggregate into large, hydrophobic columns parallel to the hexagonal axis. There are two types of columns, with either two-fold or six-fold screw symmetry, but although the calculated density is low by peptide standards,  $1.124 \text{ g cm}^{-3}$ , neither has a significant open channel at the center as is observed for the Val-Ala class, Figure 1.

From crystallization of amino acids it is well known that racemic aqueous solutions normally give rise to racemic crystals, meaning that no enantiomeric separation takes place during crystallization (although Asn [11] and allo-Ile [12] constitute interesting exceptions). The propensity to form mixed D/L-crystals has been furthermore utilized in crystallization of pseudoracemic mixtures of L- and D-amino acid, e.g. Leu and D-Val [13]. No co-crystals of this type are, however, known for a mixture of a L-L dipeptide and a D-amino acid (or vice versa). As part of a student project we decided to investigate this option by setting up a series of crystallization experiments for such mixtures. None of these in fact produced co-crystals, but one of the test tubes, containing a mixture of Leu-Ile and D-Leu, yielded a new crystal form for the dipeptide. Subsequent X-ray structure determination showed the structure to be Leu-Ile  $2.5\text{H}_2\text{O}$  (I), the first example of a new type of a nanoporous peptide material, described in detail here.

## MATERIALS AND METHODS

### Crystal Growth

Leu-Ile was obtained from Bachem, while amino acids were obtained from Sigma. Peptide crystals were grown by vapor

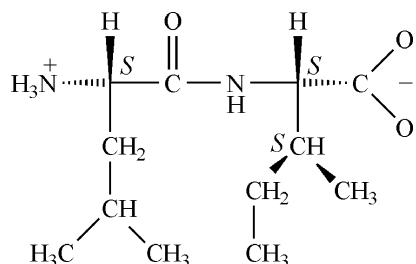
\*Correspondence to: Carl Henrik Görbitz, Department of Chemistry, University of Oslo, Blindern, N-0315 OSLO, Norway; e-mail: c.h.gorbitz@kjemi.uio.no

<sup>‡</sup>This article is part of the Special Issue of the Journal of Peptide Science entitled "Peptides in Nanotechnology".

diffusion of acetonitrile into an aqueous solution containing an equimolar mixture of the peptide and the amino acid, total mass  $\sim 1$  mg.

### X-ray Diffraction

Reflections were measured on a Siemens SMART 1000 CCD-diffractometer using  $\text{MoK}\alpha$  radiation ( $\lambda = 0.71069 \text{ \AA}$ ). The data collection with SMART [14] at 105 K included five sets of exposures, two with the detector set at  $2\theta = 26^\circ$  and three



**Scheme 1** Schematic drawing of Leu-Ile.

at  $2\theta = 55^\circ$ , crystal-to-detector distance 5.0 cm. Data integration and cell refinement with SAINT [15], absorption correction by SADABS [16], structure solution by direct methods and subsequent full-matrix least-squares refinement on  $F^2$  with SHELXTL [17]. Positional parameters were refined for H-atoms bonded to O and N, other H-atoms were positioned with idealized geometry and fixed C-H distances in the range 0.98–1.00  $\text{\AA}$ .  $U_{\text{iso}}$  values were 1.2  $U_{\text{eq}}$  of the carrier atom or 1.5  $U_{\text{eq}}$  for amino and methyl groups as well as water molecules. In the absence of significant anomalous scattering effects, 7636 Friedel pairs were merged. Leu-Ile hydrate:  $\text{C}_{12}\text{H}_{24}\text{N}_2\text{O}_3 \cdot 2.5\text{H}_2\text{O}$ ,  $M = 289.37$ , orthorhombic,  $P2_12_12_1$ ,  $a = 10.7633(4) \text{ \AA}$ ,  $b = 10.9482(4) \text{ \AA}$ ,  $c = 28.0887(10) \text{ \AA}$ ,  $V = 3309.9(2) \text{ \AA}^3$ ,  $Z = 8$ ,  $N_{\text{measured}} = 52591$ ,  $N_{\text{unique}} = 9518$ ,  $N_{\text{observed}} [F^2 > 2\sigma(F^2)] = 8886$ , parameters = 414,  $R_{\text{int}} = 0.026$ ,  $R[F^2 > 2\sigma(F^2)] = 0.029$ ,  $wR(F^2) = 0.080$ , CCDC 649962.

### NMR

NMR-spectra were collected for three different samples: (i) fresh material from the jar, (ii) a set of about ten bulky crystals for which single crystal structure determination had

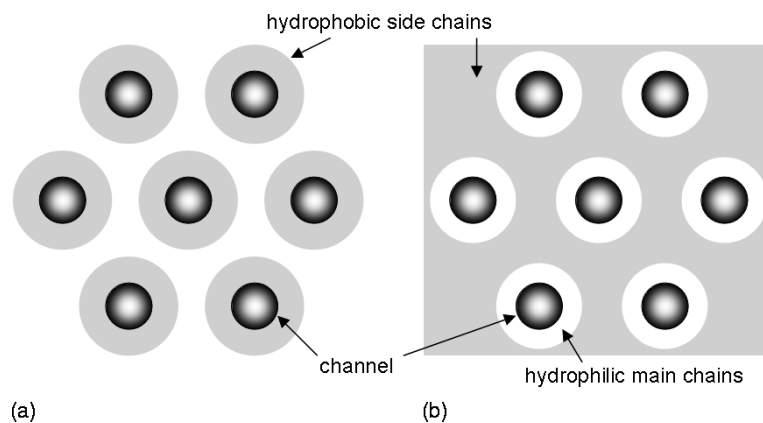


**Figure 1** Schematic drawing showing the two different modes of separating hydrophilic and hydrophobic moieties in crystal structures belonging to (a) the Val-Ala class with hydrophobic column and (b) the Phe-Phe class with a hydrophobic 3-D matrix.

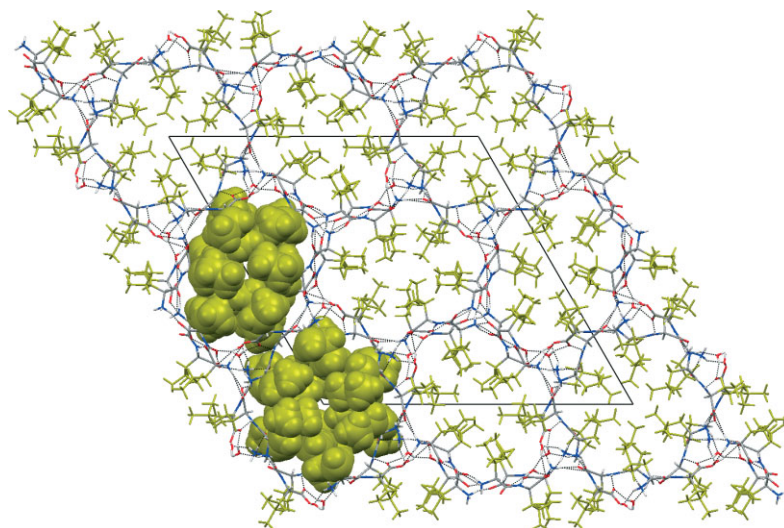


**Figure 2** The unit cell and crystal packing arrangement of Leu-Ile-0.75 hydrate. Side chains have been colored in orange; hydrogen bonds are shown as dotted lines. For two columns side chains have been depicted in a spacefill representation.

failed, (iii) wool-like precipitate from a test tube containing the dipeptide together with succinic acid.

The samples were each dissolved in 9:1 H<sub>2</sub>O : D<sub>2</sub>O (0.5 ml) in Wilmad 5 mm NMR tubes (535-PP). The NMR experiments were performed on a Bruker AV600 NMR instrument operating at 600.13 MHz. The module Topshim was used for shimming. Tuning and matching was performed with the semiautomatic program 'ATMM'. Optimal presat solvent suppression was selected automatically with the BioTool automation program controlling the TopSpin software. The standard pulse program hsqcetf3gpsi delivered with the software package TopSpin 2.0 was used for acquisition. The 2D experiments were performed with 256 indirect increments with 2 or 4 scans per increment

depending upon the amount of available substance. The acquisition times were 10 and 20 min, respectively. The data sets were processed and plotted with TopSpin 2.0.

## RESULTS

The crystal structure of (I), with two peptide molecules and five water molecules in the asymmetric unit, is shown in Figure 3. All bond lengths and bond angles are normal. Torsion angles are listed in Table 1 while hydrogen-bonding parameters are given in Table 2.

**Table 1** Selected torsion angles (°)

Molecule A		Molecule B		
N1A—C1A—C6A—N2A	133.10 (6)	N1B—C1B—C6B—N2B	116.24 (7)	$\psi_1$
C1A—C6A—N2A—C7A	169.51 (6)	C1B—C6B—N2B—C7B	176.94 (6)	$\omega_1$
C6A—N2A—C7A—C12A	-125.97 (7)	C6B—N2B—C7B—C12B	-107.07 (7)	$\varphi_2$
N2A—C7A—C12A—O2A	-5.19 (9)	N2B—C7B—C12B—O2B	-74.80 (8)	$\psi_T$
N1A—C1A—C2A—C3A	-176.75 (7)	N1B—C1B—C2B—C3B	-175.79 (6)	$\chi_1^1$
C1A—C2A—C3A—C4A	62.65 (9)	C1B—C2B—C3B—C4B	57.94 (9)	$\chi_1^{2,1}$
C1A—C2A—C3A—C5A	-174.21 (7)	C1B—C2B—C3B—C5B	-179.37 (7)	$\chi_1^{2,2}$
N2A—C7A—C8A—C9A	62.04 (7)	N2B—C7B—C8B—C9B	-61.85 (7)	$\chi_2^{1,1}$
N2A—C7A—C8A—C11A	-62.58 (8)	N2B—C7B—C8B—C11B	174.67 (6)	$\chi_2^{1,2}$
C7A—C8A—C9A—C10A	174.18 (7)	C7B—C8B—C9B—C10B	160.25 (8)	$\chi_2^2$

**Table 2** Hydrogen-bonding geometry (Å, °)

D—H...A	D—H	H...A	D...A	D—H...A
N1A—H1A...O1W	0.900 (14)	1.812 (14)	2.7036 (9)	170.3 (13)
N1A—H2A...O3B	0.927 (14)	1.891 (13)	2.7993 (8)	166.2 (13)
N1A—H3A...O2B <sup>a</sup>	0.927 (14)	1.942 (14)	2.8524 (8)	166.9 (13)
N2A—H4A...O3W	0.795 (14)	2.301 (14)	3.0596 (9)	159.9 (13)
N1B—H1B...O3A <sup>b</sup>	0.894 (14)	1.830 (15)	2.7242 (8)	179.7 (16)
N1B—H2B...O2W	0.868 (14)	2.123 (14)	2.8889 (9)	146.8 (13)
N1B—H3B...O2B <sup>c</sup>	0.899 (14)	2.124 (14)	2.8899 (8)	142.6 (12)
N2B—H4B...O3B <sup>c</sup>	0.837 (13)	1.964 (13)	2.7873 (8)	167.3 (12)
O1W—H11W...O3A <sup>d</sup>	0.888 (18)	1.953 (17)	2.8267 (9)	167.8 (16)
O1W—H12W...O5W <sup>b</sup>	0.870 (17)	1.840 (17)	2.7103 (10)	178.8 (18)
O2W—H21W...O1A <sup>c</sup>	0.857 (17)	1.955 (17)	2.7760 (9)	160.0 (16)
O2W—H22W...O2A <sup>b</sup>	0.854 (17)	1.940 (17)	2.7808 (9)	167.8 (15)
O3W—H31W...O1B	0.840 (17)	1.943 (17)	2.7532 (8)	161.7 (17)
O3W—H32W...O4W	0.869 (18)	2.214 (18)	3.0297 (12)	156.1 (16)
O4W—H41W...O2A	0.84 (2)	1.91 (2)	2.7535 (10)	174.2 (17)
O4W—H42W...O3W <sup>f</sup>	0.87 (2)	2.12 (2)	2.9671 (12)	165.1 (17)
O5W—H51W...O2W	0.85 (2)	1.95 (2)	2.7919 (10)	173.0 (19)
O5W—H52W...O4W	0.85 (2)	1.95 (2)	2.8055 (12)	176.4 (19)

Symmetry codes:

<sup>a</sup>  $x + 1/2, -y + 3/2, -z + 1$ .

<sup>b</sup>  $-x + 1, y + 1/2, -z + 3/2$ .

<sup>c</sup>  $x - 1/2, -y + 3/2, -z + 1$ .

<sup>d</sup>  $-x + 2, y + 1/2, -z + 3/2$ .

<sup>e</sup>  $x - 1, y, z$ .

<sup>f</sup>  $-x + 1, y - 1/2, -z + 3/2$ .

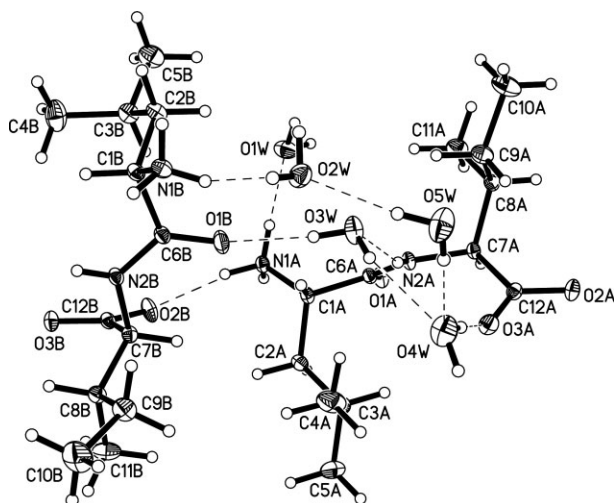


**Figure 3** The asymmetric unit of I. Displacement ellipsoids are shown at the 50% probability level and H-atoms are shown as spheres of arbitrary size. Hydrogen bonds are shown as dashed lines.

In each NMR-spectrum the NH amide cross peaks have the same  $^1\text{H}$  and  $^{15}\text{N}$  shifts; 7.90 ppm and 127.50 ppm, respectively (the values were not calibrated since no internal standard was added). The spectra are available as supplementary material.

## DISCUSSION

In the presence of D-Leu, acting as a template for crystal growth, the title dipeptide has managed to grow a completely new type of crystal structure (I) with two peptide molecules and five water molecules in the asymmetric unit, Figure 3. The two peptide molecules have slightly different semiextended main-chain conformations, as reflected by the torsion angles in Table 1. Both Leu side chains have adopted the common *trans/trans*, *gauche*-conformations for  $\chi_1^1/\chi_1^{2,1}$ ,  $\chi_1^{2,1}$ , as have two of the four Leu side chains in the 0.75 hydrate (II) [10]. The Ile side chain of molecule B has a low-energy *gauche*-/*trans*, *trans* conformation, while the *gauche*+/*gauche*-, *trans* orientation of molecule A is somewhat more uncommon.

When viewed along the *b*-axis, Figure 4(a), the crystal packing arrangement of (I) immediately reveals the presence of hydrophilic columns filled with water molecules OW1, OW2, OW4, and OW5. OW3 is nearby and completes the water network. A 90° rotation about the long *c*-axis, Figure 4(b), shows that at the same time hydrophobic groups come together and form hydrophobic columns in much the same way as observed for (II), except that in (I) each column has contributions from eight side chains; both types of columns in (II) have contributions from 12 side chains, Figure 2. From the above, it follows that a perpendicular

**Table 3** Outcome of crystallization of 1 : 1 molar ratio mixtures between Leu-Ile and various other molecules and salts

Molecule/salt	Bulky crystals (%) <sup>a</sup>	Needles (%) <sup>b</sup>	Wool-like precipitate (%)	No precipitate (%)	N <sup>c</sup>
(none)	0	100	0	0	5
Imidazole	20	80	0	0	5
Succinic acid	0	0	100	0	5
Ammonium formate	0	60	20	20	5
Gly	0	100	0	0	5
L-Ala	0	100	0	0	5
D-Ala	0	100	0	0	5
L-Val	10	90	0	0	20
D-Val	70	30	0	0	20
L-Nva	20	75	0	5	20
D-Nva	35	35	5	25	20
L-Ile	5	95	0	0	20
D-Ile	30	70	10	0	20
L-Leu	10	65	20	5	20
D-Leu	55	35	5	0	20
L-Met	0	100	0	0	20
D-Met	30	50	0	20	20
L-Phe	20	45	25	10	20
D-Phe	30	35	10	15	20

<sup>a</sup> Form I and unknown crystal form.

<sup>b</sup> Form II.

<sup>c</sup> Number of trials.

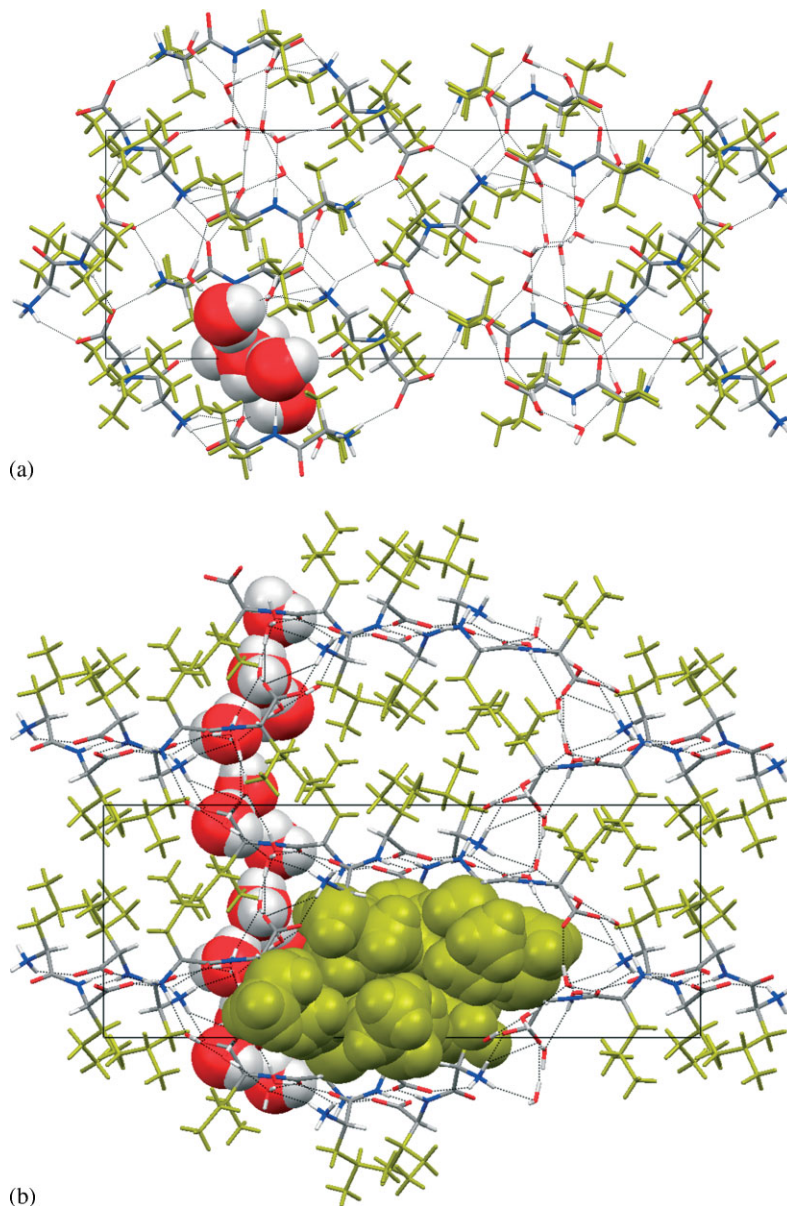


**Figure 4** The unit cell and crystal packing of I viewed along (a) the *b*-axis and (b) the *a*-axis. A column of water molecules (encompassing OW1, OW2, OW4, and OW5, but not OW3) is drawn in spacefill style, as is also a hydrophobic column of side chains in (b).

arrangement is observed for the directionalities of the channels and hydrophobic columns. Without exception, the directions of the hydrophobic aggregations and the channels have previously been found to be parallel [1], as is evident from Figure 1. The calculated density for the structure of (I),  $1.161 \text{ g cm}^{-3}$ , is directly comparable to  $1.124 \text{ g cm}^{-3}$  found for (II), which is natural as the pores are filled with water molecules. Porous structures of the Val–Ala class have reached densities as low as  $1.041 \text{ g cm}^{-3}$  for the structure of Val–Ala itself with empty channels [3].

Hydrogen bonding along a water-filled channel is shown in Figure 5. There are five water–water interactions, Table 2, and water molecule W5 interacts

with other water molecules only. Water molecules interact predominately with peptide molecule A (six interactions *vs* two for B).

The effect of D-Leu in the crystallization was investigated in some more detail by carrying out a series of crystallizations with 1:1 mixtures between Leu–Ile and enantiomers of a series of different amino acids. The results are summarized in Table 3. It turns out that crystallizations of various mixtures have essentially four easily distinguishable outcomes: needles of (II), bulky crystals, wool-like precipitation, and no (or much delayed) precipitation. With just a few of exceptions, mostly in test tubes with D-Nva, each test tube contained only crystals of one modification.

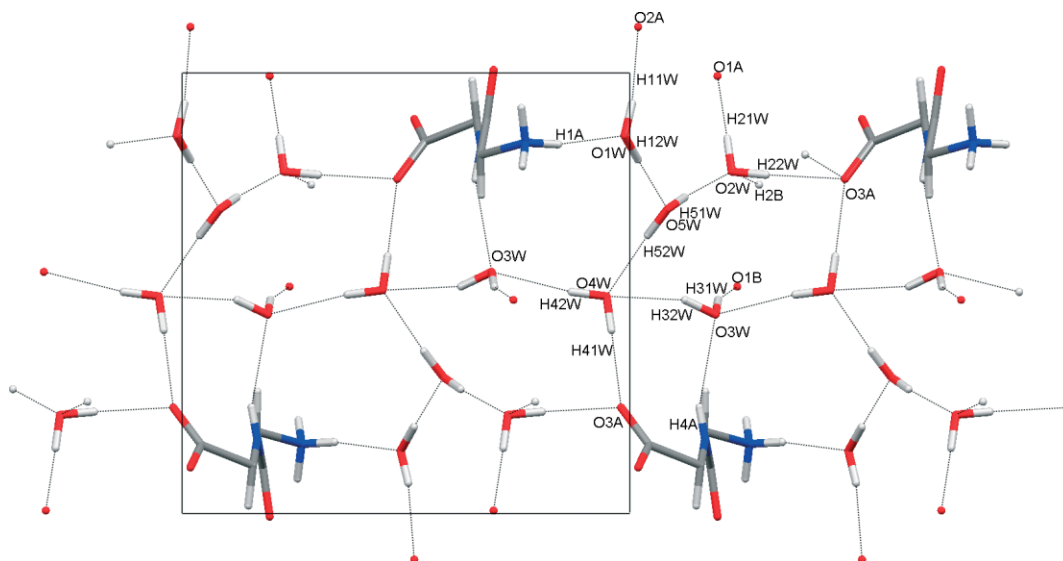


**Figure 5** Detail of the hydrogen-bonding pattern involving the co-crystallized water molecules. The view is along the *c*-axis with horizontal *b*-axis. For completeness the main chains of heavily interacting peptide molecule A molecules have been included.

The reproducibility is low, which may be partly due to instability of the title compound; observation of small bubbles in several test tubes may suggest that decarboxylation can take place. Overall, Table 3 shows that several different amino acids have the ability to shift the crystallization outcome from form (II). This includes both *L*- and *D*-amino acids, but *D*-amino acids are overall more efficient.

Crystals of (I) are easily recognized in the microscope from the rectangular shape, but the majority of the bulky crystals have a different, close to trigonal or hexagonal shape, as shown in Figure 6. X-ray data sets have been collected for three different specimens, including the one shown in Figure 6, all apparently

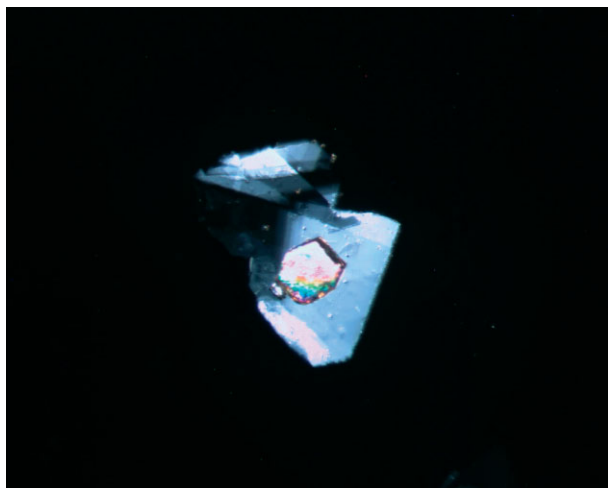


**Figure 6** Uncharacterized pseudohexagonal crystals of Leu-Ile [not form (I)] growing on a thin *D*-Leu crystal. The dimensions of the Leu-Ile crystal are approximately  $0.35 \times 0.30 \times 0.30$  mm.

belonging to the orthorhombic space group  $P2_12_12$ . The cell parameters are  $a = 10.7$ ,  $b = 11.6$ ,  $c = 36.6$  Å with quite substantial variations from one crystal to the next. All attempts to solve the crystal structure, from any of the three data sets, were fruitless. In order to establish their nature, NMR-spectra were collected for the fresh sample, for a set of bulky, hexagonally shaped crystals and also for the wool-like precipitate indicated as a possible crystallization outcome in Table 3. The fresh sample yielded, as expected, a single  $^1\text{H}/^{15}\text{N}$  2-D amide signal. A sample prepared from bulky crystals gave the very same signal, showing that cyclization into the corresponding diketopiperazine with two independent amide groups (and NMR signals) [18] had not been taking place. Accordingly, we are confident that the bulky crystals are indeed an unknown modification of Leu-Ile. This is also true for the wool-like precipitation, which also reproduced the same NMR signal.

### Supplementary Material

Supplementary electronic material for this paper is available in Wiley InterScience at: <http://www.interscience.wiley.com/jpages/1075-2617/suppmat/>

### REFERENCES

1. Görbitz CH. Microporous organic materials from hydrophobic dipeptides. *Chem. Eur. J.* 2007; **13**: 1022–1031.
2. Görbitz CH, Gundersen E. *L*-Valyl-*L*-alanine. *Acta Crystallogr. Sect. C* 1996; **52**: 1764–1767.
3. Görbitz CH. An exceptionally stable peptide nanotube system with flexible pores. *Acta Crystallogr. Sect. B* 2002; **58**: 849–854.
4. Görbitz CH. Nanotubes from hydrophobic dipeptides: Pore size regulation through side chain substitution. *N. J. Chem.* 2003; **27**: 1789–1793.

5. Görbitz CH. Nanotube formation by hydrophobic dipeptides. *Chem. Eur. J.* 2001; **7**: 5153–5159.
6. Görbitz CH. Nanotubes of L-isoleucyl-L-leucine 0.91 hydrate. *Acta Crystallogr. Sect. E* 2004; **60**: o626–o628.
7. Reches R, Gazit E. Casting metal nanowires within discrete self-assembled peptide nanotubes. *Science* 2003; **300**: 625–628.
8. Song Y, Challa SR, Medforth CJ, Qiu Y, Watt RK, Peña D, Miller JE, van Swol F, Shelnutt JA. Synthesis of peptide-nanotube platinum-nanoparticle composites. *Chem. Commun.* 2004; 1044–1045.
9. Görbitz CH, Gundersen E. L-Leu-L-Val<sup>3</sup>/4 H<sub>2</sub>O: A hexagonal crystal structure with Z = 24. *Acta Chem. Scand.* 1996; **50**: 537–543.
10. Görbitz CH. L-Leucyl-L-isoleucine 0.75 hydrate. *Acta Crystallogr. Sect. E* 2004; **60**: o647–o650.
11. Piutti A. Sur une nouvelle espèce d'asparagine. *CR. Hebd. Acad. Sci.* 1886; 134–138.
12. Dalhus B, Görbitz CH. Structural relationships in crystals accommodating different stereoisomers of 2-amino-3-methylpentanoic acid. *Acta Crystallogr. Sect. B* 2000; **56**: 720–727.
13. Dalhus B, Görbitz CH. Molecular aggregation in selected crystalline 1 : 1 complexes of hydrophobic D- and L-amino acids. III. The L-leucine and L-valine series. *Acta Crystallogr. Sect. C* 1999; **55**: 1547–1555.
14. SMART, Version 5.054. Bruker AXS Inc: Madison, Wisconsin, 1998.
15. SAINT+, Version 6.22. Bruker AXS Inc: Madison, Wisconsin, 2001.
16. Sheldrick GM. SADABS. University of Göttingen: Germany, 1996.
17. SHELXTL, Version 6.10. Bruker AXS Inc: Madison, Wisconsin, 2000.
18. Kricheldorf HR. Nitrogen-15 NMR spectroscopy. 19. Spectroscopic characterization of cyclodipeptides (2,5-dioxopiperazines). *Org. Magn. Reson.* 1980; **13**: 52–58.